

Causal Negative Sampling via Diffusion Model for Out-of-Distribution Recommendation

Chu Zhao

Northeastern University

Shenyang, China

chuzhao@stumail.neu.edu.cn

Jianzhe Zhao

Northeastern University

Shenyang, China

zhaojz@swc.neu.edu.cn

Enneng Yang

Northeastern University

Shenyang, China

ennengyang@stumail.neu.edu.cn

Guibing Guo*

Northeastern University

Shenyang, China

guogb@swc.neu.edu.cn

Yizhou Dang

Northeastern University

Shenyang, China

yzdang@stumail.neu.edu.cn

Xingwei Wang

Northeastern University

Shenyang, China

wangxw@mail.neu.edu.cn

ABSTRACT

Heuristic negative sampling enhances recommendation performance by selecting negative samples of varying hardness levels from predefined candidate pools to guide the model toward learning more accurate decision boundaries. However, our empirical and theoretical analyses reveal that unobserved environmental confounders (e.g., exposure or popularity biases) in candidate pools may cause heuristic sampling methods to introduce false hard negatives (FHNS). These misleading samples can encourage the model to learn spurious correlations induced by such confounders, ultimately compromising its generalization ability under distribution shifts. To address this issue, we propose a novel method named Causal Negative Sampling via Diffusion (CNSDiff). By synthesizing negative samples in the latent space via a conditional diffusion process, CNSDiff avoids the bias introduced by predefined candidate pools and thus reduces the likelihood of generating FHNS. Moreover, it incorporates a causal regularization term to explicitly mitigate the influence of environmental confounders during the negative sampling process, leading to robust negatives that promote out-of-distribution (OOD) generalization. Comprehensive experiments under four representative distribution shift scenarios demonstrate that CNSDiff achieves an average improvement of **13.96%** across all evaluation metrics compared to state-of-the-art baselines, verifying its effectiveness and robustness in OOD recommendation tasks. The code is available at <https://github.com/user683/CNSDiff>.

CCS CONCEPTS

- **Do Not Use This Code → Generate the Correct Terms for Your Paper;** *Generate the Correct Terms for Your Paper*; Generate the Correct Terms for Your Paper; Generate the Correct Terms for Your Paper.

*Corresponding authors.

Permission to make digital or hard copies of all or part of this work for personal or classroom use is granted without fee provided that copies are not made or distributed for profit or commercial advantage and that copies bear this notice and the full citation on the first page. Copyrights for components of this work owned by others than the author(s) must be honored. Abstracting with credit is permitted. To copy otherwise, or republish, to post on servers or to redistribute to lists, requires prior specific permission and/or a fee. Request permissions from permissions@acm.org.

Conference acronym 'XX, June 03–05, 2018, Woodstock, NY

© 2018 Copyright held by the owner/author(s). Publication rights licensed to ACM.

ACM ISBN 978-1-4503-XXXX-X/2018/06...\$15.00

<https://doi.org/XXXXXX.XXXXXXX>

KEYWORDS

Negative Sampling, Diffusion Model, Recommender Systems, Causal Regularization

ACM Reference Format:

Chu Zhao, Enneng Yang, Yizhou Dang, Jianzhe Zhao, Guibing Guo, and Xingwei Wang. 2018. Causal Negative Sampling via Diffusion Model for Out-of-Distribution Recommendation. In *Proceedings of Make sure to enter the correct conference title from your rights confirmation email (Conference acronym 'XX)*. ACM, New York, NY, USA, 14 pages. <https://doi.org/XXXXXX.XXXXXXX>

1 INTRODUCTION

Random negative sampling [34, 37] selects negative examples randomly from the set of items that a user has not interacted with, which helps prevent model overfitting and refine the decision boundary. Therefore, it has been widely applied in recommendation systems [10, 21]. To further improve model performance, researchers have proposed various enhanced strategies over the past decade. For example, *Predefined Negative Sampling* [26, 42] fixes negative examples during data preprocessing, while *Popularity-based Negative Sampling* [28, 36] selects negative samples based on item popularity, where more popular items are more likely to be chosen. Although these methods improve the quality of negative samples, they typically rely on a fixed hardness level, making it difficult to adapt to the model's varying discriminative ability at different training stages. Consequently, negative samples may be too challenging in the early stages, hindering convergence, or too simple in later stages, providing insufficient supervision signals, which limits the further improvement of model performance. To address this issue, recent studies have focused on *Heuristic Negative Sampling* [8, 11, 20], which dynamically selects negative samples of varying hardness during training from predefined candidate pools. This approach continuously provides training signals that match the model's current capability, thereby accelerating convergence and improving recommendation performance.

Although heuristic negative sampling methods have shown strong performance in improving recommendation accuracy, our theoretical and empirical analyses reveal that their reliance on predefined candidate pools makes them vulnerable to unobserved confounders within the pool, which can lead to the inclusion of false hard negatives (FHNS) and ultimately undermine the model's generalization ability. Such samples force the model to learn spurious correlations induced by environmental factors, ultimately

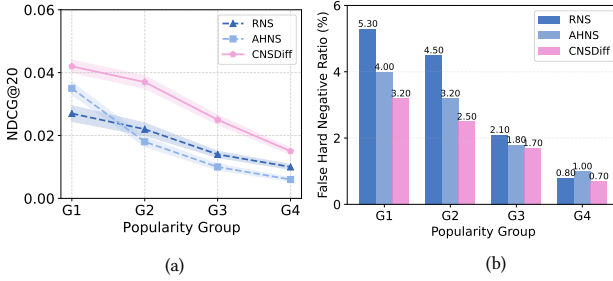


Figure 1: Performance and false hard negative ratio Across different popularity groups.

degrading its generalization performance under distribution shifts. Taking popularity as an example, low-exposure or niche items often fail to interact with users, but this does not imply that users are uninterested in them. Heuristic hard negative sampling, however, may mistakenly treat these potential positives as hard negatives that are highly similar to the user. For instance, a user may have a strong preference for an independent niche music brand, but due to its low popularity, it has never been recommended to them. Since the current embedding of such music brand is very close to this item, it is erroneously sampled as a hard negative. Compared to general false negatives, FHNS are more harmful: due to their high similarity to positive samples, the model is continuously “pushed away” from them during training, reinforcing incorrect decision boundaries. As a result, the model learns not the true preferences, but incorrectly associates “low-popularity, high-similarity items” with negative feedback. Such spurious correlations induced by popularity as a confounder severely undermine the causal robustness and out-of-distribution (OOD) generalization ability of the model. In Section 3.1, we establish a structural causal model and further illustrate our experimental findings in Figure 1: the items are grouped into four buckets according to their popularity (from high to low), and we report the performance and the ratio of false negatives in each group. The results show that AHNS suffers from performance drops in certain popularity groups, even performing worse than random negative sampling; moreover, in high-popularity groups, heuristic negative sampling produces a significantly higher false hard negative ratio. This further verifies our hypothesis that environmental confounders induce FHNS, which in turn encourage the model to learn spurious correlations and harm its OOD generalization. In Figure 6, we further illustrate the performance variations across different temporal groups and the FHNS ratio, reaching the same conclusion.

To address the above issue, we propose a novel negative sampling strategy named **CNSDiff**. Unlike traditional heuristic methods that rely on predefined candidate pools, CNSDiff takes the positive item embeddings as conditional input and leverages a diffusion model to progressively perturb them in the latent space, generating negative samples with varying hardness levels. The core intuition behind this strategy is that the initial diffusion steps preserve the semantic structure of the positive sample, while the subsequent noise injection and denoising process gradually move it away from the original distribution. This results in **high-quality hard negatives** that are close to but distinct from the positive items. We further provide the formal mathematical definition in Section 3.1. Furthermore, as illustrated in Figure 2 (a), we construct a structural causal

model (SCM) to characterize the data generation mechanism and analyze how environmental confounders may introduce spurious hard negatives, thus impairing the model’s OOD generalization capability. Based on this, we design a causal regularization term that leverages the backdoor criterion to identify and block the causal path between environmental confounders and the target variable, thereby enforcing distributional consistency of the diffusion model across different environments. This design enables CNSDiff to effectively mitigate FHNS induced by confounding factors, resulting in more robust negative sample generation. The main contributions of this work are shown as follows:

- We construct a structural causal model to reveal that environmental confounders can introduce FHNS during heuristic negative sampling, leading the model to learn spurious environment-dependent correlations and degrading its OOD generalization performance.
- We propose a diffusion-based negative sampling method with causal regularization, which utilizes the backdoor criterion in the negative sample generation process to identify and block the causal paths from environmental confounders to the target variable. This approach enforces distributional consistency of the diffusion model across environments, significantly enhancing the robustness of negative samples and the model’s generalization capability.
- Extensive experiments across various distribution shift scenarios demonstrate that our proposed method consistently outperforms baselines in terms of OOD generalization performance.

2 PRELIMINARY

2.1 Problem Formulation

In recommender systems, let the user set be $\mathcal{U} = \{u_i\}_{i=1}^M$, the item set be $\mathcal{V} = \{v_j\}_{j=1}^N$, and the user-item interaction matrix be $R \in \mathbb{R}^{M \times N}$, where $R_{uv} = 1$ indicates an interaction between user u and item v , and $R_{uv} = 0$ otherwise. Models typically learn an encoder function $f_\theta(\cdot)$ to map users and items into low-dimensional embeddings and predict user preferences based on their similarity. A widely used optimization objective is the Bayesian Personalized Ranking (BPR) loss:

$$\mathcal{L}_{\text{BPR}} = \sum_{(u, v) \in R} -\log \sigma(s(u, v) - s(u, v^-)), \quad (1)$$

where $s(u, v)$ denotes the predicted score of user u for item v , σ is the sigmoid function, and v^- represents a negatively sampled item not interacted with by the user. BPR trains the model by contrasting positive and negative samples to capture user preference. Existing methods often adopt heuristic negative sampling strategies, selecting negatives from a candidate item pool either randomly or by rule. However, such approaches are prone to introducing false hard negatives (FHNS). Through empirical analysis, we demonstrate that FHNS can amplify spurious correlations caused by environmental confounders, ultimately harming the model’s generalization to OOD scenarios. Therefore, this work aims to design a novel negative sampling strategy to mitigate the impact of FHNS and enhance the model’s OOD generalization performance.

2.2 Diffusion Model

Diffusion model [4, 49] is a class of deep generative models that have achieved significant success in computer vision due to their

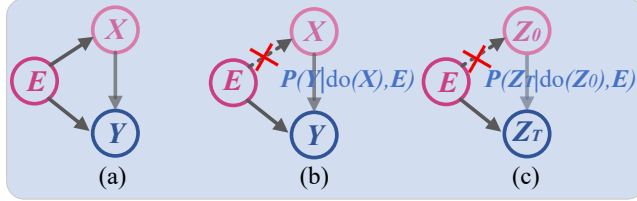


Figure 2: Causal Graph Analysis Model. E represents unobserved environmental factors, X denotes the input (i.e., user-item pairs), and Y is the model’s predicted output.

high-quality generation, training stability, and solid theoretical grounding. They consist of two key phases: a **forward process**, which progressively adds Gaussian noise to data $x_0 \sim p(x_0)$, here, $p(x_0)$ denotes the **true data distribution**, and a **reverse process**, which learns to recover the original data. In the forward process, noise is added step-by-step:

$$q(x_t|x_{t-1}) = \mathcal{N}(x_t; \sqrt{1 - \beta_t}x_{t-1}, \beta_t \cdot \mathbf{I}), \quad (2)$$

where $\beta_t \in (0, 1)$ controls the noise level at step t . \mathbf{I} is the identity matrix. The notation $\mathcal{N}(\cdot; \mu, \Sigma)$ denotes a multivariate Gaussian distribution with mean μ and covariance Σ . Thus, x_t is sampled by scaling x_{t-1} and adding zero-mean Gaussian noise with variance β_t , making the sample gradually more noisy. Using the reparameterization trick, we have:

$$q(x_t|x_0) = \mathcal{N}(x_t; \sqrt{\bar{\alpha}_t}x_0, (1 - \bar{\alpha}_t) \cdot \mathbf{I}), \quad (3)$$

where $\bar{\alpha}_t = \prod_{i=1}^t (1 - \beta_i)$. The reverse process learns a denoising model $p_\theta(x_{t-1}|x_t)$ parameterized by neural networks:

$$p_\theta(x_{t-1}|x_t) = \mathcal{N}(x_{t-1}; \mu_\theta(x_t, t), \Sigma_\theta(x_t, t)). \quad (4)$$

Training minimizes the variational lower bound (VLB):

$$\mathcal{L}_{\text{VLB}} = \mathbb{E}_q \left[\sum_{t=1}^T \text{KL}(q(x_{t-1}|x_t, x_0) \| p_\theta(x_{t-1}|x_t)) \right] - \log p_\theta(x_0|x_1), \quad (5)$$

which is often simplified to a mean squared error (MSE) loss on noise prediction:

$$\mathcal{L}_{\text{sampling}} = \mathbb{E}_{t, x_0, \epsilon} \left[\|\epsilon - \epsilon_\theta(\sqrt{\bar{\alpha}_t}x_0 + \sqrt{1 - \bar{\alpha}_t}\epsilon, t)\|^2 \right]. \quad (6)$$

This reformulation not only improves training stability but also enables efficient optimization using standard regression techniques. In our setting, the diffusion model enables controllable synthesis of negative samples by varying the diffusion step $T = \{0 \leq t \leq T\}$. Smaller T yields harder negatives closer to the original item x_0 , while larger T produces easier negatives with more noise. This provides a principled way to generate negatives of varying hardness in continuous space, without relying on heuristic candidate sets.

3 METHODOLOGY

We now present our analysis and the proposed model. In Section 3.1, we construct a causal structural model (SCM) to characterize the data generation process, illustrating how false hard negatives (FHNS) are introduced and how they amplify spurious correlations that undermine out-of-distribution generalization. Section 3.3 details the diffusion-based mechanism for synthesizing negative samples with controllable hardness. In Section 3.4, we introduce a causal regularization term that mitigates the influence of

confounding factors during negative sampling. Finally, we provide a time complexity analysis and discuss why CNSDiff is effective.

3.1 Causal Analysis for Negative Sampling

To investigate the impact of FHNS on the out-of-distribution (OOD) generalization of models, we conduct a causal analysis to uncover the dependencies among key variables in the recommendation process. Our analysis reveals that FHNS amplify spurious correlations introduced by environment-specific factors, thereby degrading model robustness under distribution shifts. We construct the SCM (Figure 2), where E denotes the environment, X represents the user-item input pair, and Y is the model’s predicted output. The causal dependencies are characterized as follows:

- $E \rightarrow X$: The environment influences the exposure distribution $p(X | E)$, introducing biases such as popularity or temporal shift.
- $X \rightarrow Y$: The model deterministically maps X to prediction via $Y = f_\theta(X)$.
- $E \rightarrow Y$: Although not directly modeled, this path is implicitly introduced by environment-biased negative sampling during training.

We first provide the mathematical definition of FHNS:

Definition 3.1 (False Hard Negative Sample). In the presence of environmental confounders, certain user-preferred items may have low exposure probability and remain unobserved. Let $Y_{u,v} \in \{0, 1\}$ denote the true preference of user u for item v , and $\phi(v, e)$ denote the exposure probability of item v under environment e . A sample (u, v) is defined as a **False Hard Negative Sample (FHNS)** if:

$$\text{FHNS}_{u,v} := \{\tilde{Y}_{u,v} = 0 \mid Y_{u,v} = 1, \phi(v, e) \ll 1, \text{sim}(z_u, z_v) \geq \tau\}, \quad (7)$$

where $\tilde{Y}_{u,v} = 0$ is the sampled label observed as a negative, $Y_{u,v} = 1$ indicates a true preference of user u for item v , $\phi(v, e) \ll 1$ denotes a low exposure probability of item v under environment e , and $\text{sim}(z_u, z_v) \geq \tau$ implies high semantic similarity between the user and item embeddings, exceeding a threshold τ . Such false negatives mislead the model by incorrectly penalizing relevant items, potentially amplifying spurious correlations and impairing generalization under distribution shifts.

These FHNS are often indistinguishable from true positives in the representation space, thereby introducing high-magnitude noise during training. The BPR loss in Eq. (1) can be further expressed as:

$$\mathcal{L}_{\text{BPR}}(\theta) = -\mathbb{E}_{(u, v, v^-) \sim \mathcal{D}} [\log \sigma(f_\theta(u, v) - f_\theta(u, v^-))], \quad (8)$$

when the sampled negative v^- is actually a false hard negative (i.e., $\tilde{Y}_{u,v^-} = 0$ but $Y_{u,v^-} = 1$) and \mathcal{D} is the dataset, the model is misled to push a truly relevant item away from the user in the embedding space. This misoptimization distorts the learned decision boundary and significantly degrades recommendation performance, especially under distribution shift. We define the **environment-conditioned false hard negative rate** as:

$$\eta(e) := P(\tilde{Y} = 0 \mid Y = 1, E = e), \quad (9)$$

which captures the probability that true positives are mislabeled as negatives under environment e . As a result, the model learns a weighted version of the true label distribution:

$$f_\theta(X) \approx \mathbb{E}[\tilde{Y} \mid X = x] = \mathbb{E}_E [P(Y = 1 \mid X, E) \cdot (1 - \eta(E))], \quad (10)$$

This implies a spurious dependence of prediction on E even when X is fixed, leading to overfitting to environment-specific artifacts and degraded OOD generalization. We further elaborate in Theorem 3.2 how FHNS amplify spurious correlations.

THEOREM 3.2 (FALSE HARD NEGATIVES AMPLIFY ENVIRONMENT-INDUCED SPURIOUS CORRELATIONS). *Suppose the false hard negative rate $\eta(e)$ varies across environments $e \in E$, and the model $f_\theta(x)$ is differentiable with respect to a latent variable z_E aligned with the environmental variable E . If the test environment distribution $P_{\text{test}}(E)$ differs from the training distribution $P_{\text{train}}(E)$, then the generalization gap admits the following lower bound:*

$$\mathcal{L}_{\text{test}}(f_\theta) - \mathcal{L}_{\text{train}}(f_\theta) \geq \gamma \cdot \text{TV}(P_{\text{train}}(E), P_{\text{test}}(E)) + \varepsilon_{\text{inv}}. \quad (11)$$

where $\text{TV}(P_{\text{train}}(E), P_{\text{test}}(E)) = \frac{1}{2} \int |P_{\text{train}}(e) - P_{\text{test}}(e)| de$ is the total variation distance between the training and test environment distributions, $\gamma = \mathbb{E}_X \left[\left\| \frac{\partial f_\theta(X)}{\partial z_E} \right\| \right] \cdot \text{Var}_e(\eta(e))$ quantifies the model's sensitivity to environment-specific false negative perturbations, and ε_{inv} captures the irreducible invariant risk. A complete proof is provided in Appendix A.1.

3.2 Negative Sampling via Diffusion

Inspired by [23], we take the generated item embeddings as the input to the diffusion model and extract the embeddings from multiple time steps to implement a hierarchical generative negative sampling strategy. Specifically, CNSDiff controls the difficulty of negative samples by adjusting the diffusion time step T . For instance, when $T = 0$, the generated embeddings are from the final stage of the diffusion process and are the hardest to distinguish from positive samples in the latent space, thus regarded as the *hardest negatives*. In contrast, embeddings generated at earlier diffusion steps (i.e., larger T) tend to be easier to distinguish from positives. In general, the time step T serves as a proxy for the hardness of negative samples: the smaller the T , the more challenging the negative samples. Specifically, taking graph-based collaborative filtering as an example, given a user-item interaction pair $\langle u, i \rangle$, we first construct an interaction graph G . Then, a graph convolutional network is employed to obtain the user embeddings z_u and item embeddings z_v , respectively. The positive item embeddings z_v are subsequently used as the input to the diffusion model. The overall processing pipeline is illustrated as follows:

$$z_v \rightarrow z_0 \xrightarrow{\phi} \cdots z_t \xrightarrow{\psi} \hat{z}_{t-1} \cdots \xrightarrow{\psi} \hat{z}_0, \quad (12)$$

where ϕ represents injecting noise into the input embedding, while ψ removes the noise through optimization. \hat{z}_0 represents the denoised embedding. CNSDiff controls both the quantity and hardness of the generated negative samples by selecting outputs from specific diffusion time steps between 0 and T . The embedding at time step T can be obtained as follows:

$$p_\theta(x_{t-1} | x_t) = \frac{1}{\sqrt{\alpha_t}} \left(x_t - \frac{1 - \alpha_t}{\sqrt{1 - \bar{\alpha}_t}} \right) + \sqrt{\beta_t} \cdot \mathbf{I}. \quad (13)$$

Through the above sampling strategy, CNSDiff constructs a set of generated negative samples with different levels of *hardness*, denoted as $\{h_t \mid 0 < t < T\}$. In practice, the choice of diffusion time steps has a significant impact on both the quality of negative samples and training efficiency. Smaller time steps (i.e., those closer

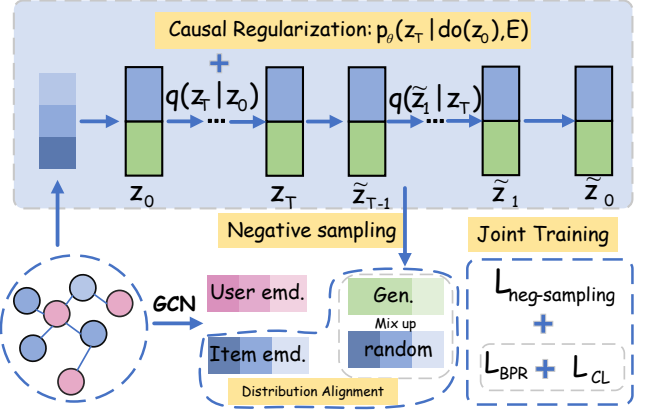


Figure 3: Illustration of the proposed CNSDiff architecture. The model takes the item embeddings as input and synthesizes a set of robust negative samples with varying levels of hardness via diffusion-based causal regularization. These samples are then integrated with random negatives through mixup and aligned semantically, enabling a joint training framework that enhances the generalization.

to $t = 0$) tend to produce more challenging negatives, but at the cost of increased computational overhead. In contrast, larger time steps may generate easily distinguishable negatives that provide limited learning signals for the model. To strike a balance between training efficiency and the diversity of generated negative samples, we adopt a uniformly spaced sampling strategy across the diffusion process. Instead of using all intermediate steps, we select a subset of representative time steps to generate negatives, thereby covering samples with different levels of semantic hardness while reducing computational cost. We define the set of sampling steps as:

$$\mathcal{D}_{h_t} = \{h_t \mid t = t_0 + k \cdot s, t \leq T, k \in \mathbb{N}\}, \quad (14)$$

where t_0 denotes the initial step, s is the stride (i.e., interval between sampled steps), and T is the total number of diffusion steps. This strategy ensures both sampling efficiency and sufficient coverage of varying negative sample difficulty.

3.3 Optimization with Causal Regularization

As discussed in Section 3.1, FHNS can amplify spurious correlations introduced by environmental variables, thereby undermining the model's out-of-distribution generalization ability. The aforementioned diffusion-based negative sampling methods do not explicitly address environmental confounders, and thus struggle to achieve robust generalization. Inspired by recent advances, a feasible solution is to perform deconfounded modeling by estimating the interventional distribution: $p_\theta(Y \mid \text{do}(X), E)$, which aims to block the dependency path from the environment variable E to the input feature X , and consequently uncover stable and transferable causal relationships between X and Y . In the following, we explore how to explicitly learn causally invariant user preference representations during the negative sample generation process using diffusion models, with the goal of enhancing generalization under distribution shifts. Given an initial embedding z_0 , the generative process under an unobserved environment variable $E = e$ can be modeled as a

conditional diffusion chain:

$$p_\theta(z_T | z_0, E = e) = \prod_{t=0}^{T-1} p_\theta(z_{t+1} | z_t, e), \quad (15)$$

where z_0 denotes the starting point of the diffusion process and T is the total number of diffusion steps. The corresponding log-likelihood can be expressed as:

$$\log p_\theta(z_T | z_0, E = e) = \sum_{t=0}^{T-1} \log p_\theta(z_{t+1} | z_t, e). \quad (16)$$

To eliminate the influence of unobserved confounding factors on negative sample generation and simultaneously capture user preferences that are invariant across environments, an ideal approach is to adopt deconfounder learning. This can be formulated as modeling the interventional distribution: $p_\theta(z_T | \text{do}(z_0), E = e)$, where the do-operator removes spurious associations induced by environment-dependent confounding. We present the following theory directly.

THEOREM 3.3. *For a given diffusion model $p_\theta(z_T | z_0, e)$, which models the generation of latent representations conditioned on both the initial embedding and environment variable, the deconfounded learning objective admits the following variational lower bound:*

$$\log p_\theta(z_T | \text{do}(z_0), E = e) \geq \sum_{t=0}^{T-1} \mathbb{E}_{q_\phi(e|z_t)} \left[\log \frac{p_\theta(z_{t+1} | z_t, e) p_0(e)}{q_\phi(e | z_t)} \right], \quad (17)$$

where $q_\phi(e | z_t)$ is a variational approximation of the posterior over environment variables, and $p_0(e)$ denotes the prior over environments.

The proof is deferred to Appendix A.2. Notably, the variational objective can be interpreted as an importance reweighting mechanism, where the ratio. $\frac{p_0(e)}{p(e|z_t)}$ adjusts for the imbalance in the distribution of the environment variable. This reweighting down-plays dominant environments and emphasizes under-represented ones, thereby mitigating the observation bias induced by skewed or limited training data. Consequently, the model learns more stable and invariant transitions. $z_t \rightarrow z_{t+1}$ generalizes beyond the training distribution. Overall, this variational formulation facilitates effective deconfounding in generative representation learning by explicitly modeling and correcting for latent environmental confounders. Based on Eq. (17), we propose a diffusion-based negative sampling objective with causal regularization:

$$\mathcal{L}_{\text{neg_sampling}} = \mathcal{L}_{\text{sampling}} + \lambda_1 \cdot \log p_\theta(z_T | \text{do}(z_0), E), \quad (18)$$

where $\mathcal{L}_{\text{sample}}$ denotes the sampling loss from generated negatives, λ_1 is a penalty coefficient. This regularization encourages the model to eliminate spurious correlations introduced by confounding factors and to learn stable representations across varying environments. We provide the full derivation of the causal regularization term in Appendix A.3.

3.4 Joint Training

After obtaining the set of negative samples \mathcal{D}_h generated by the diffusion model, we follow previous work and select the most informative negative sample by computing the similarity between each generated item and the user embedding. Specifically, we choose the

generated sample with the highest inner product score with the user embedding z_u :

$$e_h = \arg \max_{h_t \in \mathcal{D}_h} (z_u \cdot h_t), \quad (19)$$

where h_t denotes a generated candidate from \mathcal{D}_h . This ensures that e_h is the most attractive (i.e., hard) negative sample for the user, which enhances the difficulty and informativeness of the learning signal. To improve training stability and generalization, we further introduce a progressive interpolation strategy that mixes the selected hard negative e_h with a randomly sampled negative e_r to construct the final negative embedding:

$$\tilde{e} = \alpha \cdot e_r + \beta \cdot e_h, \quad (20)$$

where α and β are interpolation weights, and dynamically evolve with training process. In the early stages of training, we assign a higher weight to randomly sampled negatives ($\alpha > \beta$) to encourage diversity and exploration. As training progresses, we gradually increase the contribution of the generated negatives ($\beta > \alpha$), allowing the model to focus on more challenging and informative examples. This curriculum-inspired mixing strategy balances easy and hard samples over time, improving both robustness and OOD generalization. Furthermore, to enhance the discriminability of the generated negatives in the item embedding space, we adopt a contrastive learning objective. The contrastive loss is formally defined as follows:

$$\mathcal{L}_{\text{CL}} = -\log \frac{\exp \left(\frac{z_0 \cdot z_j}{\tau} \right)}{\exp \left(\frac{z_0 \cdot z_j}{\tau} \right) + \sum_{k \neq j} \exp \left(\frac{z_0 \cdot \bar{e}_k}{\tau} \right)}, \quad (21)$$

where z_j denotes the embeddings of the anchor and its positive counterpart, respectively, and τ is a temperature parameter that controls the concentration of similarity scores. The negative samples in the denominator include both generated and randomly sampled items. We adopt a joint optimization framework to train the model:

$$\mathcal{L}_{\text{total}} = \mathcal{L}_{\text{BPR}} + \lambda_2 \cdot \mathcal{L}_{\text{neg_sampling}} + \lambda_3 \cdot \mathcal{L}_{\text{CL}}, \quad (22)$$

where λ_2 and λ_3 are hyperparameters that control the contribution of the negative sampling and contrastive loss terms, respectively. The model architecture is illustrated in Figure 3, and the algorithm pseudocode is presented in Algorithm 1.

3.5 Time Complexity

In LightGCN, the time complexity of neighborhood aggregation and embedding update is $O(K \cdot |E| \cdot d)$. K is the number of graph convolution layers, E is the number of edges, and d is the dimensionality of the embeddings. With the introduction of the diffusion-based for negative sampling, each positive sample requires the generation of M negative samples via a diffusion process with T steps, where each step incurs a computation cost of $O(d^2)$. Therefore, the overall time complexity of negative sampling becomes $O(N_{\text{pos}} \cdot M \cdot T \cdot d^2)$ where N_{pos} is the number of positive user-item pairs in the training data. The total training complexity is: $O(K \cdot |E| \cdot d + N_{\text{pos}} \cdot M \cdot T \cdot d^2)$. Additionally, we benchmark the per-epoch runtime of CNSDiff against other state-of-the-art negative sampling methods, as shown in Table 6. CNSDiff demonstrates superior efficiency compared to MixGCF and AHNS, highlighting its scalability during training.

Table 1: Performance comparison of CNSDiff with state-of-the-art baselines under distribution shift scenarios on the Yelp2018, KuaiRec, and Food datasets. We report Recall@K (R@K) and NDCG@K (N@K) as evaluation metrics. The best results are highlighted in bold, and the second-best results are underlined.

Methods	Yelp2018				KuaiRec				Food			
	R@10	N@10	R@20	N@20	R@10	N@10	R@20	N@20	R@10	N@10	R@20	N@20
RNS (SIGIR'20)	0.0033	0.0020	0.0079	0.0036	0.0742	0.5096	0.1120	0.4268	0.0233	0.0182	0.0404	0.0242
DNS(M, N) (WWW'23)	0.0014	0.0006	0.0128	0.0036	0.0529	0.3111	0.0829	0.2658	0.0146	0.0107	0.0274	0.0150
MixGCF (KDD'22)	0.0027	0.0016	0.0078	0.0034	0.0541	0.3341	0.0963	0.2856	0.0162	0.0113	0.0295	0.0158
AHNS (AAAI'24)	0.0008	0.0005	0.0032	0.0013	0.0526	0.3097	0.0829	0.2651	0.0151	0.0101	0.0304	0.0154
DMNS (WWW'24)	0.0006	0.0003	0.0012	0.0005	0.0760	0.5078	0.1074	0.4300	0.0275	0.0201	0.0463	0.0272
InvCF (WWW'23)	0.0016	0.0008	0.0013	0.0008	0.0871	0.2021	0.1024	0.2083	0.0030	0.0012	0.0033	0.0013
AdvInfoNCE (NIPS'23)	0.0047	0.0024	0.0083	0.0038	0.0744	0.4109	0.0985	0.4020	0.0227	0.0135	0.0268	0.0159
CDR (TOIS'23)	0.0011	0.0006	0.0016	0.0008	0.0570	0.2630	0.0860	0.2240	0.0260	0.0195	0.0412	0.0254
DR-GNN (WWW'24)	0.0044	0.0029	0.0076	0.0041	0.0808	0.5326	0.1066	0.4511	0.0246	0.0205	0.0436	0.0272
DiffRec (SIGIR'23)	0.0007	0.0004	0.0016	0.0007	0.0011	0.0158	0.0023	0.0128	0.0036	0.0029	0.0078	0.0050
HDRM (WWW'25)	0.0025	0.0017	0.0046	0.0024	0.0410	0.2742	0.0645	0.2332	0.0141	0.0117	0.0257	0.0165
CausalDiff (WWW'25)	0.0077	0.0049	0.0130	0.0068	0.0880	0.5410	0.1132	0.4523	0.0285	0.0209	0.0471	0.0278
CNSDiff (Ours)	0.0101	0.0069	0.0163	0.0091	0.0909	0.5572	0.1384	0.4678	0.0304	0.0225	0.0496	0.0290
Improv. %	+31.69%	+40.82%	+25.38%	+33.82%	+3.59%	+2.99%	+2.23%	+3.42%	+6.31%	+7.66%	+5.31%	+4.32%

3.6 Discussion

This section analyzes **why the negative samples synthesized by CNSDiff can improve the model’s OOD generalization ability**. Existing studies [23, 38] have pointed out that an ideal negative sample distribution p_{v^-} should exhibit a *sub-linear positive correlation* with the positive sample distribution p_v , i.e., it should satisfy $p_{v^-} \propto p_v^\alpha$, where $0 < \alpha < 1$. Furthermore, existing work [23] theoretically proves that under a properly designed diffusion modeling setup, the distribution of negative samples naturally adheres to this sub-linear positivity principle. As a result, negative samples synthesized by diffusion models tend to exhibit strong training performance and generalization ability. However, it is important to note that this theoretical foundation relies on the assumption of a stable data distribution, which may not hold in real-world scenarios with distribution shift. As demonstrated by the results of DMNS in Table 1 and the ablation setting CNSDiff w/o All in Table 2, failure to account for latent *environmental confounders* can lead to diffusion-generated negative samples being influenced by spurious factors, thereby impairing OOD performance. To address this issue, we extend the above theoretical framework by introducing a *causal regularization* term, which explicitly enforces environment-invariance during the diffusion process. This constraint effectively mitigates the impact of confounders and further enhances the robustness and generalization capability of the model under distribution shifts.

4 EXPERIMENT

We conduct extensive experiments to evaluate the effectiveness of CNSDiff and aim to address the following key scientific questions: **(RQ1)** How does CNSDiff perform compared to state-of-the-art (SOTA) negative sampling methods? Can it enhance model generalization in the face of distributional shifts? **(RQ2)** How do the individual components of CNSDiff contribute to the performance?

(RQ3) How do different hyperparameter settings of CNSDiff affect its OOD generalization capability? **(RQ4)** What is the potential of CNSDiff in mitigating the challenges of false hard negative samples (FHNS) problem?

Datasets. Following prior work [12,13], we evaluate the performance of CNSDiff under three representative distribution shift scenarios: popularity shift, temporal shift, and exposure shift. Experiments are conducted on three widely used benchmark datasets: Food, KuaiRec, and Yelp2018. Comprehensive details about the datasets and preprocessing procedures are provided in Appendix B.

Baselines. We compare CNSDiff with three categories of SOTA baselines: (1) **Negative sampling methods**: RNS [10], DNS (M, N) [25], MixGCF [8], AHNS [11], and DMNS [23]. (2) **Distribution shift-aware methods**: InvCF [41], AdvInfoNCE [40], CDR [29], and DR-GNN [27]. (3) **Diffusion-based methods**: DiffRec [30], HDRM [39], and CausalDiff [45]. Detailed descriptions of these baselines are provided in Appendix B. The hyperparameter configurations for CNSDiff are outlined in Appendix C.

4.1 Overall Performance (RQ1)

Based on the results shown in Table 1, we derive the following key observations: **(1) CNSDiff significantly outperforms existing SOTA heuristic negative sampling methods under distribution shift scenarios.** Specifically, when compared to the top-performing heuristic method, MixGCF, CNSDiff demonstrates a notable performance improvement across multiple evaluation metrics on both the KuaiRec and Food datasets, and also demonstrates substantial gains on the Yelp2018 dataset. These results validate the effectiveness of CNSDiff in enhancing the OOD generalization ability of recommendation models. We mainly attribute this significant performance gain to two fundamental components of CNSDiff:

- **Diffusion-based negative sample generation**, which breaks away from the limitations of traditional heuristic sampling methods

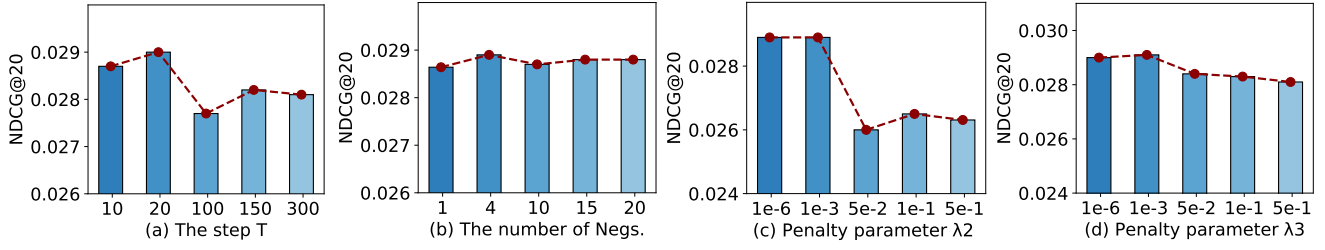


Figure 4: Evaluating the impact of model hyperparameter sets on recommendation performance.

that rely on pre-defined candidate sets. Instead, it allows sampling of negative items with varying hardness levels from the diffusion process, thus reducing the likelihood of false negative samples.

- **Causal Regularization:** This component explicitly mitigates the influence of spurious correlations introduced by environment-related confounders during model training. By incorporating a causal regularization term into the objective function, it effectively blocks the erroneous causal pathways through which false negative samples could otherwise reinforce and amplify such misleading correlations. As a result, the framework not only enhances the stability of the learned representations but also promotes better generalization by enforcing invariance across different environmental conditions

Moreover, we observe that heuristic negative sampling methods generally fail to maintain strong OOD generalization under diverse types of distribution shifts. This further supports our motivation: *heuristic strategies tend to introduce false hard negatives, which mislead the model into learning spurious patterns and consequently harm its generalization performance.* (2) **CNSDiff also consistently outperforms existing SOTA OOD generalization methods and diffusion-based baselines.** Concretely, CNSDiff achieves an average performance gain of 13.96% across multiple datasets. We attribute this improvement to its unique use of **causal regularization during the negative sampling phase.** Unlike prior methods, CNSDiff explicitly models both the latent environment confounders and the negative sample generation process, enabling it to (i) mitigate the misleading effects of unobserved environment variables and (ii) synthesize high-quality negative samples with varying levels of robustness. This mechanism compels the model to learn more accurate and robust decision boundaries, which in turn leads to stronger generalization performance under distribution shifts.

4.2 Ablation Study

This section presents ablation studies to validate the effectiveness of each module in CNSDiff. Specifically, **CNSDiff w/o Mixup** removes the interpolation between diffusion-generated and randomly sampled negatives. **CNSDiff w/o Align.** eliminates the embedding alignment between generated negatives and original items. **CNSDiff w/o Causal** disables the causal regularization designed to mitigate the influence of unobserved confounders. **CNSDiff w/o All** removes all three components simultaneously. The results are summarized in Table 2. We observe the following insights: (1) Removing the Mixup module consistently degrades performance across datasets, confirming its role in enhancing training robustness by increasing sample diversity. (2) Disabling embedding alignment leads to even greater performance drops in most cases, indicating

Table 2: Ablation Study on Three Datasets.

Dataset	Method	R@10	N@20	R@20	N@20
Food	CNSDiff w/o Mixup	0.0291	0.0218	0.0480	0.0285
	CNSDiff w/o Align.	0.0280	0.0217	0.0482	0.0284
	CNSDiff w/o Causal	0.0290	0.0212	0.0480	0.0286
	CNSDiff w/o All	0.0275	0.0201	0.0463	0.0279
	CNSDiff	0.0300	0.0222	0.0490	0.0300
Yelp2018	CNSDiff w/o Mixup	0.0020	0.0012	0.0033	0.0016
	CNSDiff w/o Align.	0.0018	0.0011	0.0025	0.0014
	CNSDiff w/o Causal	0.0018	0.0011	0.0028	0.0015
	CNSDiff w/o All	0.0015	0.0005	0.0018	0.0010
	CNSDiff	0.0101	0.0069	0.0163	0.0091
KuaiRec	CNSDiff w/o Mixup	0.0892	0.5460	0.1329	0.4697
	CNSDiff w/o Align.	0.0798	0.5299	0.1225	0.4569
	CNSDiff w/o Causal	0.0888	0.5518	0.1340	0.4681
	CNSDiff w/o All	0.0760	0.5078	0.1174	0.4300
	CNSDiff	0.0909	0.5572	0.1384	0.4781

that maintaining semantic consistency between generated and real items is vital for learning reliable decision boundaries. (3) Omitting causal regularization also results in performance decline, validating its effectiveness in suppressing spurious correlations and improving generalization under distribution shifts. (4) The removal of all three modules leads to the worst overall performance, demonstrating that Mixup, alignment, and causal regularization function complementarily and are jointly critical to CNSDiff’s success. These results collectively underscore the necessity of each component in achieving strong performance, particularly in OOD scenarios.

4.3 Hyperparameter Analysis (RQ3)

To thoroughly evaluate the robustness and sensitivity of our proposed model, we conduct a comprehensive ablation study on several key hyperparameters, as illustrated in Figure 4. Our key analyses and conclusions are as follows:

- **Diffusion step T:** This parameter controls how far the sampling process explores in the latent space. We observe that the performance initially improves with larger T , peaking around $T = 20$, and then gradually degrades. This suggests that a moderate diffusion depth enables the model to generate sufficiently diverse yet semantically meaningful negatives. However, excessive diffusion

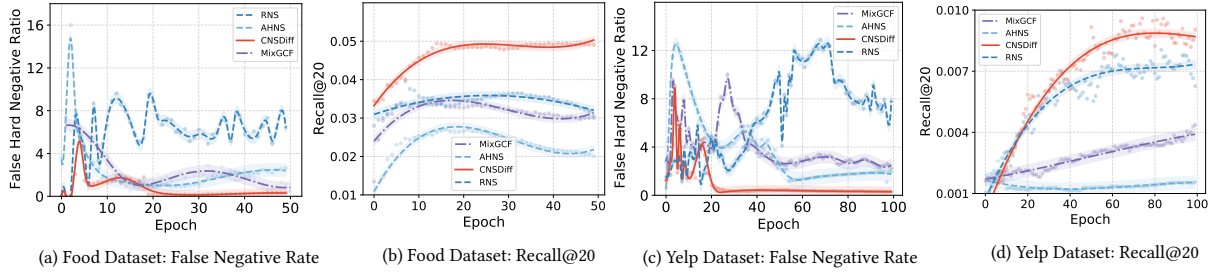


Figure 5: False Negative Rate and Recall@20 Metric Over Epochs for Different-based Negative sampling.

(e.g., $T > 100$) leads to noisy or overly distant samples, which impede learning and increase computational overhead.

- **Number of negative samples:** The model maintains stable performance across a range of negative sample counts, with optimal results achieved when using 5 to 10 negatives per positive instance. This indicates that incorporating multiple hard negative views benefits learning, though the marginal gain saturates as the number increases further. However, an excessive number of negative samples will also increase computational costs. In practice, a balance must be struck between computational overhead and performance.
- **Regularization coefficient λ_3 (for diffusion sampling):** This penalty controls the semantic difficulty of sampled negatives. Small values (e.g., $1e-6$ to $1e-3$) yield better performance, while large penalties (e.g., $\geq 5e-2$) significantly hurt NDCG. This highlights the importance of balancing diversity and semantic consistency.
- **Regularization coefficient λ_3 .** We observe a similar trend: moderate regularization improves generalization, while overly strong constraints reduce embedding expressiveness. Mild semantic alignment helps enforce meaningful representations without overfitting.

Furthermore, in Table 5, we further investigate the impact of different choices of alpha and beta on model performance. Overall, Best performance is achieved with a diffusion step $T \approx 20$, using 5–10 negatives per positive sample, and applying mild regularization on both sampling and contrastive alignment losses.

4.4 False Negative Analysis of CNSDiff (RQ4)

To evaluate the effectiveness of CNSDiff in mitigating FHNS, we measure the proportion of false negatives among generated negative samples at each epoch. A sample is considered a false negative if its cosine similarity with any test item exceeds 0.99. Experiments are conducted on the Food and Yelp datasets, and the results are shown in Figure 5. We summarize the key observations as follows: (1) CNSDiff substantially reduces the false hard negative ratio compared to heuristic sampling methods. This advantage stems from its diffusion-based generation mechanism, which avoids relying on fixed candidate pools that often include near-duplicate positives. Notably, the false negative ratio is relatively high in the early training stages due to the predominance of random sampling before the diffusion-based negatives are fully integrated. (2) CNSDiff achieves faster convergence and better performance, further validating the effectiveness of the causal regularization term. By suppressing spurious correlations introduced by FHNS, the model gains stronger generalization ability under distribution shifts.

5 RELATED WORK

5.1 Negative Sampling in Recommendation

Negative sampling is a widely adopted technique for training recommendation models [21, 22]. Over the past decade, various strategies have been proposed to improve training efficiency and performance, such as random negative sampling [7, 24, 44, 47], popularity-based sampling [43, 51], and predefined sampling methods [42, 50]. Most of these fall under static strategies, where negative samples remain fixed during training, limiting the ability to mine informative hard negatives. To address this, dynamic sampling approaches have emerged that select semantically similar negatives from candidate pools [2, 3, 5, 20, 38], interpolate between positives to generate harder negatives [8, 11], or synthesize high-quality samples via generative models like GANs [6]. With the rise of large language models (LLMs), recent work has explored LLM-generated semantic negatives to enhance generalization [48]. Distinct from these methods, our work revisits the negative sampling paradigm by highlighting the risk of false negatives introduced by heuristic sampling. Such samples can amplify spurious correlations unrelated to user preference, thereby degrading model generalization under distribution shift.

5.2 Diffusion-based Recommendation

Owing to their powerful generative and representation learning capabilities, diffusion models have achieved significant success across a range of generative tasks [1, 4, 33], spurring the development of various diffusion-based recommendation approaches [15, 31]. Existing works can be broadly categorized into three directions:

Data augmentation and robust representation learning: Diffusion models are used to enhance robustness via noise-injection and denoising, benefiting tasks like sequential recommendation [9, 16, 19, 32], graph-based modeling [45, 46], and social network denoising [12, 14, 49].

Generative modeling core: Some works adopt diffusion models as the primary mechanism for simulating user-item interactions, enabling direct modeling of preferences or rankings [17, 30].

Personalized content generation: Diffusion models are also used to generate user-conditioned content, such as personalized images or product styles in creative recommendation settings [18, 35]. Different from above, we explore a novel perspective that leverages diffusion models to synthesize negative samples of varying hardness. Our goal is to mitigate the impact of confounders and enhance both training effectiveness and out-of-distribution generalization for ID-based recommendation models. In Appendix E, we further discuss the distinctions between our approach and existing diffusion-based recommendation methods.

6 CONCLUSION

In this work, we propose CNSDiff, a causal negative sampling framework leveraging diffusion models to improve recommendation robustness under distribution shifts. Unlike traditional sampling methods prone to false negatives, CNSDiff synthesizes negatives in the latent space with causal regularization and hardness control, mitigating spurious correlations and enhancing out-of-distribution generalization. Extensive experiments on three real-world datasets confirm CNSDiff's consistent superiority over strong baselines. Ablation studies further validate the effectiveness of the proposed components. This work highlights the potential of integrating generative modeling and causal inference for robust recommendation. Future work will explore theoretical foundations and extensions to multi-modal and online recommendation.

REFERENCES

- [1] Hanqun Cao, Cheng Tan, Zhangyang Gao, Yilun Xu, Guangyong Chen, Pheng-Ann Heng, and Stan Z Li. 2024. A survey on generative diffusion models. *TKDE* (2024).
- [2] Chong Chen, Weizhi Ma, Min Zhang, Chenyang Wang, Yiqun Liu, and Shaoping Ma. 2023. Revisiting negative sampling vs. non-sampling in implicit recommendation. *TOIS* 41, 1 (2023), 1–25.
- [3] Xiao Chen, Wenqi Fan, Jingfan Chen, Haochen Liu, Zitao Liu, Zhaoxiang Zhang, and Qing Li. 2023. Fairly adaptive negative sampling for recommendations. In *WWW*. 3723–3733.
- [4] Florinel-Alin Croitoru, Vlad Hondu, Radu Tudor Ionescu, and Mubarak Shah. 2023. Diffusion models in vision: A survey. *TPAMI* 45, 9 (2023), 10850–10869.
- [5] Jingtao Ding, Yuhua Quan, Quanming Yao, Yong Li, and Depeng Jin. 2020. Simplify and robustify negative sampling for implicit collaborative filtering. *NIPS* 33 (2020), 1094–1105.
- [6] Guibing Guo, Huan Zhou, Bowei Chen, Zhirong Liu, Xiao Xu, Xu Chen, Zhenhua Dong, and Xiuqiang He. 2020. IPGAN: Generating informative item pairs by adversarial sampling. *TNNLS* 33, 2 (2020), 694–706.
- [7] Xiangnan He, Lizi Liao, Hanwang Zhang, Liqiang Nie, Xia Hu, and Tat-Seng Chua. 2017. Neural collaborative filtering. In *WWW*. 173–182.
- [8] Tinglin Huang, Yuxiao Dong, Ming Ding, Zhen Yang, Wenzheng Feng, Xinyu Wang, and Jie Tang. 2021. Mixgef: An improved training method for graph neural network-based recommender systems. In *KDD*. 665–674.
- [9] Yangqin Jiang, Yuhao Yang, Lianghao Xia, and Chao Huang. 2024. Diffkg: Knowledge graph diffusion model for recommendation. In *WSDM*. 313–321.
- [10] Yehuda Koren, Robert Bell, and Chris Volinsky. 2009. Matrix factorization techniques for recommender systems. *Computer* 42, 8 (2009), 30–37.
- [11] Riwei Lai, Rui Chen, Qilong Han, Chi Zhang, and Li Chen. 2024. Adaptive hardness negative sampling for collaborative filtering. In *AAAI*, Vol. 38. 8645–8652.
- [12] Anchen Li and Bo Yang. 2025. Dual Graph Denoising Model for Social Recommendation. In *WWW*. 347–356.
- [13] Zihao Li, Aixin Sun, and Chenliang Li. 2023. Diffurec: A diffusion model for sequential recommendation. *TOIS* 42, 3 (2023), 1–28.
- [14] Zongwei Li, Lianghao Xia, and Chao Huang. 2024. Recdiff: diffusion model for social recommendation. In *CIKM*. 1346–1355.
- [15] Jianghao Lin, Jiaqi Liu, Jiachen Zhu, Yunjia Xi, Chengkai Liu, Yangtian Zhang, Yong Yu, and Weinan Zhang. 2024. A Survey on Diffusion Models for Recommender Systems. *arXiv* (2024).
- [16] Qidong Liu, Fan Yan, Xiangyu Zhao, Zhaocheng Du, Huifeng Guo, Ruiming Tang, and Feng Tian. 2023. Diffusion augmentation for sequential recommendation. In *CIKM*. 1576–1586.
- [17] Shuo Liu, An Zhang, Guoqing Hu, Hong Qian, and Tat-seng Chua. 2024. Preference Diffusion for Recommendation. *arXiv* (2024).
- [18] Zhi Lu, Yang Hu, Yan Chen, and Bing Zeng. 2021. Personalized outfit recommendation with learnable anchors. In *CVPR*. 12722–12731.
- [19] Haokai Ma, Ruobing Xie, Lei Meng, Xin Chen, Xu Zhang, Leyu Lin, and Zhanhui Kang. 2024. Plug-in diffusion model for sequential recommendation. In *AAAI*, Vol. 38. 8886–8894.
- [20] Haokai Ma, Ruobing Xie, Lei Meng, Xin Chen, Xu Zhang, Leyu Lin, and Jie Zhou. 2023. Exploring false hard negative sample in cross-domain recommendation. In *Recsys*. 502–514.
- [21] Haokai Ma, Ruobing Xie, Lei Meng, Fuli Feng, Xiaoyu Du, Xingwu Sun, Zhanhui Kang, and Xiangxu Meng. 2024. Negative Sampling in Recommendation: A Survey and Future Directions. *arXiv* (2024).
- [22] Tiroshan Madushanka and Ryutaro Ichise. 2024. Negative sampling in knowledge graph representation learning: A review. *arXiv* (2024).
- [23] Trung-Kien Nguyen and Yuan Fang. 2024. Diffusion-based negative sampling on graphs for link prediction. In *WWW*. 948–958.
- [24] Steffen Rendle, Christoph Freudenthaler, Zeno Gantner, and Lars Schmidt-Thieme. 2012. BPR: Bayesian personalized ranking from implicit feedback. *arXiv* (2012).
- [25] Wentao Shi, Jiawei Chen, Fuli Feng, Jizhi Zhang, Junkang Wu, Chongming Gao, and Xiangnan He. 2023. On the theories behind hard negative sampling for recommendation. In *WWW*. 812–822.
- [26] Dongjin Song, David A Meyer, and Dacheng Tao. 2015. Efficient latent link recommendation in signed networks. In *KDD*. 1105–1114.
- [27] Bohao Wang, Jiawei Chen, Changdong Li, Sheng Zhou, Qihao Shi, Yang Gao, Yan Feng, Chun Chen, and Can Wang. 2024. Distributionally Robust Graph-based Recommendation System. In *WWW*. 3777–3788.
- [28] Hongwei Wang, Fuzheng Zhang, Miao Zhao, Wenjie Li, Xing Xie, and Minyi Guo. 2019. Multi-task feature learning for knowledge graph enhanced recommendation. In *The world wide web conference*. 2000–2010.
- [29] Wenjie Wang, Xinyu Lin, Liuhui Wang, Fuli Feng, Yunshan Ma, and Tat-Seng Chua. 2023. Causal disentangled recommendation against user preference shifts. *TOIS* 42, 1 (2023), 1–27.
- [30] Wenjie Wang, Yiyuan Xu, Fuli Feng, Xinyu Lin, Xiangnan He, and Tat-Seng Chua. 2023. Diffusion recommender model. In *SIGIR*. 832–841.
- [31] Ting-Ruen Wei and Yi Fang. 2025. Diffusion Models in Recommendation Systems: A Survey. *arXiv* (2025).
- [32] Zihao Wu, Xin Wang, Hong Chen, Kaidong Li, Yi Han, Lifeng Sun, and Wenwu Zhu. 2023. Diff4rec: Sequential recommendation with curriculum-scheduled diffusion augmentation. In *ACM MM*. 9329–9335.
- [33] Zhen Xing, Qijun Feng, Haoran Chen, Qi Dai, Han Hu, Hang Xu, Zuxuan Wu, and Yu-Gang Jiang. 2024. A survey on video diffusion models. *Comput. Surveys* 57, 2 (2024), 1–42.
- [34] Lanling Xu, Jianxun Lian, Wayne Xin Zhao, Ming Gong, Linjun Shou, Daxin Jiang, Xing Xie, and Ji-Rong Wen. 2022. Negative sampling for contrastive representation learning: A review. *arXiv* (2022).
- [35] Yiyuan Xu, Wenjie Wang, Fuli Feng, Yunshan Ma, Jizhi Zhang, and Xiangnan He. 2024. Diffusion models for generative outfit recommendation. In *SIGIR*. 1350–1359.
- [36] Yonghui Yang, Le Wu, Kun Zhang, Richang Hong, Hailin Zhou, Zhiqiang Zhang, Jun Zhou, and Meng Wang. 2023. Hyperbolic graph learning for social recommendation. *TKDE* 36, 12 (2023), 8488–8501.
- [37] Zhen Yang, Ming Ding, Tinglin Huang, Yukuo Cen, Junshuai Song, Bin Xu, Yuxiao Dong, and Jie Tang. 2024. Does negative sampling matter? a review with insights into its theory and applications. *TPAMI* 46, 8 (2024), 5692–5711.
- [38] Zhen Yang, Ming Ding, Chang Zhou, Hongxia Yang, Jingren Zhou, and Jie Tang. 2020. Understanding negative sampling in graph representation learning. In *WSDM*. 1666–1676.
- [39] Meng Yuan, Yutian Xiao, Wei Chen, Chou Zhao, Deqing Wang, and Fuzhen Zhuang. 2025. Hyperbolic diffusion recommender model. In *WWW*. 1992–2006.
- [40] An Zhang, Leheng Sheng, Zhibo Cai, Xiang Wang, and Tat-Seng Chua. 2024. Empowering collaborative filtering with principled adversarial contrastive loss. *NIPS* 36 (2024).
- [41] An Zhang, Jingnan Zheng, Xiang Wang, Yancheng Yuan, and Tat-Seng Chua. 2023. Invariant collaborative filtering to popularity distribution shift. In *Proceedings of the ACM Web Conference 2023*. 1240–1251.
- [42] Tao Zhang, Luwei Yang, Zhibo Xiao, Wen Jiang, and Wei Ning. 2024. On practical diversified recommendation with controllable category diversity framework. In *WWW*. 255–263.
- [43] Weinan Zhang, Tianqi Chen, Jun Wang, and Yong Yu. 2013. Optimizing top-n collaborative filtering via dynamic negative item sampling. In *SIGIR*. 785–788.
- [44] Yihao Zhang, Chu Zhao, Weiwen Liao, Wei Zhou, and Meng Yuan. 2023. Asymmetrical attention networks fused autoencoder for debiased recommendation. *TIST* 14, 6 (2023), 1–24.
- [45] Chu Zhao, Enneng Yang, Yuliang Liang, Pengxiang Lan, Yuting Liu, Jianzhe Zhao, Guibing Guo, and Xingwei Wang. 2025. Graph representation learning via causal diffusion for out-of-distribution recommendation. In *WWW*. 334–346.
- [46] Chu Zhao, Enneng Yang, Yuliang Liang, Jianzhe Zhao, Guibing Guo, and Xingwei Wang. 2025. Distributionally robust graph out-of-distribution recommendation via diffusion model. In *WWW*. 2018–2031.
- [47] Chu Zhao, Enneng Yang, Yuliang Liang, Jianzhe Zhao, Guibing Guo, and Xingwei Wang. 2025. Symmetric Graph Contrastive Learning against Noisy Views for Recommendation. *TOIS* 43, 3 (2025), 1–28.
- [48] Chu Zhao, Enneng Yang, Yuting Liu, Jianzhe Zhao, Guibing Guo, and Xingwei Wang. 2025. Can LLM-Driven Hard Negative Sampling Empower Collaborative Filtering? Findings and Potentials. *arXiv* (2025).
- [49] Juju Zhao, Wang Wenjie, Yiyuan Xu, Teng Sun, Fuli Feng, and Tat-Seng Chua. 2024. Denoising diffusion recommender model. In *SIGIR*. 1370–1379.
- [50] Guanjie Zheng, Fuzheng Zhang, Zihan Zheng, Yang Xiang, Nicholas Jing Yuan, Xing Xie, and Zhenhui Li. 2018. DRN: A deep reinforcement learning framework for news recommendation. In *WWW*. 167–176.

[51] Ziwei Zhu, Yun He, Xing Zhao, Yin Zhang, Jianling Wang, and James Caverlee. 2021. Popularity-opportunity bias in collaborative filtering. In *WSDM*. 85–93.

A PROOF AND DERIVATION

A.1 The Proof of Theorem 3.1

We analyze the generalization gap between the training loss under corrupted labels and the test loss under true labels. Let the training and test objectives be defined as:

$$\mathcal{L}_{\text{train}}(f_\theta) = \mathbb{E}_{(X, \tilde{Y}) \sim P_{\text{train}}} [\ell(f_\theta(X), \tilde{Y})], \quad (23)$$

$$\mathcal{L}_{\text{test}}(f_\theta) = \mathbb{E}_{(X, Y) \sim P_{\text{test}}} [\ell(f_\theta(X), Y)]. \quad (24)$$

Assume the noisy label \tilde{Y} is generated via environment-dependent false negative process:

$$P(\tilde{Y} = 1 \mid X) = \mathbb{E}_E [P(Y = 1 \mid X, E)(1 - \eta(E))], \quad (25)$$

where $\eta(E) := P(\tilde{Y} = 0 \mid Y = 1, E)$ is the false negative rate conditioned on environment variable E . Suppose the model takes the form $f_\theta(X) = g(X) + \lambda h(z_E)$, where z_E is a latent representation influenced by E (e.g., item popularity). Using a first-order Taylor expansion, we approximate:

$$\ell(f_\theta(X), \tilde{Y}) \approx \ell(f_\theta(X), Y) - \eta(E)P(Y = 1 \mid X, E) \cdot \frac{\partial \ell}{\partial f_\theta}. \quad (26)$$

Taking expectation over P_{train} , we have:

$$\begin{aligned} \mathcal{L}_{\text{train}}(f_\theta) &\approx \mathbb{E}_{(X, E) \sim P_{\text{train}}} [\ell(f_\theta(X), Y)] \\ &\quad - \mathbb{E}_{(X, E) \sim P_{\text{train}}} \left[\eta(E)P(Y = 1 \mid X, E) \cdot \frac{\partial \ell}{\partial f_\theta} \right]. \end{aligned} \quad (27)$$

Hence, the generalization gap becomes:

$$\begin{aligned} \mathcal{L}_{\text{test}}(f_\theta) - \mathcal{L}_{\text{train}}(f_\theta) &\approx \mathbb{E}_{(X, E) \sim P_{\text{test}}} [\ell(f_\theta(X), Y)] \\ &\quad - \mathbb{E}_{(X, E) \sim P_{\text{train}}} [\ell(f_\theta(X), Y)] \\ &\quad + \mathbb{E}_{(X, E) \sim P_{\text{train}}} \left[\eta(E)P(Y = 1 \mid X, E) \cdot \frac{\partial \ell}{\partial f_\theta} \right]. \end{aligned} \quad (28)$$

We focus on the environment-induced shift. Note that:

$$\mathbb{E}_{P_{\text{test}}} [f_\theta(X)] - \mathbb{E}_{P_{\text{train}}} [f_\theta(X)] = \lambda \cdot (\mathbb{E}_{P_{\text{test}}} [h(z_E)] - \mathbb{E}_{P_{\text{train}}} [h(z_E)]). \quad (29)$$

Assuming h is L_h -Lipschitz, the total variation inequality yields:

$$|\mathbb{E}_{P_{\text{test}}} [h(z_E)] - \mathbb{E}_{P_{\text{train}}} [h(z_E)]| \leq L_h \cdot \text{TV}(P_{\text{train}}(E), P_{\text{test}}(E)). \quad (30)$$

We define the environment sensitivity of f_θ as:

$$\gamma := \mathbb{E}_X \left[\left\| \frac{\partial f_\theta(X)}{\partial z_E} \right\| \right] \cdot \text{Var}_E(\eta(E)). \quad (31)$$

Combining all terms, we obtain the following lower bound on the generalization gap:

$$\mathcal{L}_{\text{test}}(f_\theta) - \mathcal{L}_{\text{train}}(f_\theta) \geq \gamma \cdot \text{TV}(P_{\text{train}}(E), P_{\text{test}}(E)) + \varepsilon_{\text{inv}}, \quad (32)$$

where ε_{inv} denotes the residual irreducible error due to noise and approximation limits.

A.2 Proof of Theorem 3.2: Variational Lower Bound for Deconfounded Learning Objective

We aim to derive a variational lower bound for the deconfounded learning objective $\log p_\theta(z_T \mid \text{do}(z_0), E)$, where z_0 is the initial embedding, z_T is the negative sample generated via a diffusion model, and E is the environment with discrete states e . The diffusion model is defined by the transition probabilities $p_\theta(z^{(l+1)} \mid z^{(l)}, e)$, and the goal is to learn causal relationships robust to distribution shifts.

Do-Calculus Rules

We use two fundamental rules of do-calculus (Pearl et al., 2016) for a causal DAG with nodes Z_0 , Z_T , and E :

- (1) **Action/Observation Exchange:**

$$P(z_T \mid \text{do}(z_0), \text{do}(e)) = P(z_T \mid \text{do}(z_0), e), \quad \text{if } (Z_T \perp E \mid Z_0)_{A_{Z_0 E}}$$

- (2) **Insertion/Deletion of Actions:**

$$P(z_T \mid \text{do}(z_0), \text{do}(e)) = P(z_T \mid \text{do}(z_0)), \quad \text{if } (Z_T \perp E \mid Z_0)_{A_{Z_0 E}}$$

Derivation of the Deconfounded Objective

The deconfounded objective is:

$$p_\theta(z_T \mid \text{do}(z_0), E) = \sum_e p_\theta(z_T \mid \text{do}(z_0), e, E) p(e \mid \text{do}(z_0))$$

Using the do-calculus rules:

- By the action/observation exchange rule, assuming $(Z_T \perp E \mid Z_0, e)_{A_{Z_0 E}}$:

$$p_\theta(z_T \mid \text{do}(z_0), e, E) = p_\theta(z_T \mid z_0, e, E)$$

- By the insertion/deletion rule, assuming $(E \perp Z_0)_{A_{Z_0}}$:

$$p(e \mid \text{do}(z_0)) = p_0(e)$$

Thus:

$$p_\theta(z_T \mid \text{do}(z_0), E) = \sum_e p_\theta(z_T \mid z_0, e, E) p_0(e) = \mathbb{E}_{p_0(e)} [p_\theta(z_T \mid z_0, e, E)]$$

For the diffusion model, we have:

$$p_\theta(z_T \mid z_0, e, E) = \prod_{l=0}^{T-1} p_\theta(z_{t+1} \mid z_t, e)$$

The log-likelihood is:

$$\log p_\theta(z_T \mid \text{do}(z_0), E) = \log \sum_{z_1, \dots, z_{T-1}} \sum_e \prod_{l=0}^{T-1} p_\theta(z_{t+1} \mid z_t, e) p_0(e)$$

Variational Lower Bound

To derive the lower bound, we introduce a variational distribution $q_\phi(e \mid z_t)$ to approximate the posterior of e . We split the derivation into intermediate steps ($t = 0, \dots, T-2$) and the final step ($t = T-1$).

Intermediate Steps ($t = 0, \dots, T-2$). For each term:

$$\log \sum_{z_{t+1}} \sum_e p_\theta(z_{t+1} | z_t, e) p_0(e)$$

Rewrite using $q_\phi(e | z_t)$:

$$\log \sum_{z_{t+1}} \sum_e \left[p_\theta(z_{t+1} | z_t, e) p_0(e) \frac{q_\phi(e | z_t)}{q_\phi(e | z_t)} \right]$$

Applying Jensen's inequality:

$$\begin{aligned} &\geq \sum_e q_\phi(e | z_t) \cdot \log \left[\sum_{z_{t+1}} \frac{p_\theta(z_{t+1} | z_t, e) p_0(e)}{q_\phi(e | z_t)} \right] \\ &= \mathbb{E}_{q_\phi(e | z_t)} \left[\log \frac{p_\theta(z_{t+1} | z_t, e) p_0(e)}{q_\phi(e | z_t)} \right]_{z_{t+1}} \end{aligned}$$

where we use $\sum_{z_{t+1}} p_\theta(z_{t+1} | z_t, e) = 1$.

Final Step ($t = T-1$). For the final step:

$$\begin{aligned} &\log \sum_e p_\theta(z_T | z_{T-1}, e) p_0(e) \\ &= \log \sum_e \left[p_\theta(z_T | z_{T-1}, e) p_0(e) \frac{q_\phi(e | z_{T-1})}{q_\phi(e | z_{T-1})} \right] \\ &\geq \mathbb{E}_{q_\phi(e | z_{T-1})} \left[\log \frac{p_\theta(z_T | z_{T-1}, e) p_0(e)}{q_\phi(e | z_{T-1})} \right] \end{aligned}$$

Combined Result. Combining the results, we obtain:

$$\log p_\theta(z_T | \text{do}(z_0), E) \geq \sum_{t=0}^{T-1} \mathbb{E}_{q_\phi(e | z_t)} \left[\log \frac{p_\theta(z_{t+1} | z_t, e) p_0(e)}{q_\phi(e | z_t)} \right]$$

The marginalization over z_1, \dots, z_{T-1} is implicit through the delta predictive distribution $p_\theta(z_{t+1} | z_t, e)$.

Equality Condition

Equality holds in Jensen's inequality if the function inside the expectation is constant with respect to e . For each step:

$$p_\theta(z^{(l+1)} | z^{(l)}, e) p_0(e) = c \cdot q_\phi(e | z^{(l)})$$

Summing over e :

$$\sum_{z^{(l+1)}} \sum_e p_\theta(z^{(l+1)} | z^{(l)}, e) p_0(e) = c \cdot \sum_e q_\phi(e | z^{(l)}) = c$$

Thus:

$$q_\phi(e | z^{(l)}) = \frac{p_\theta(z^{(l+1)} | z^{(l)}, e) p_0(e)}{\sum_{z^{(l+1)}} \sum_{e'} p_\theta(z^{(l+1)} | z^{(l)}, e') p_0(e')}$$

Since:

$$p(e | z^{(l+1)}, z^{(l)}) = \frac{p_\theta(z^{(l+1)} | z^{(l)}, e) p(e | z^{(l)})}{\sum_{e'} p_\theta(z^{(l+1)} | z^{(l)}, e') p(e' | z^{(l)})}$$

Assuming $p(e | z^{(l)}) = p_0(e)$, we have:

$$q_\phi(e | z^{(l)}) = p(e | z^{(l+1)}, z^{(l)}) \cdot \frac{p_0(e)}{p(e | z^{(l)})}$$

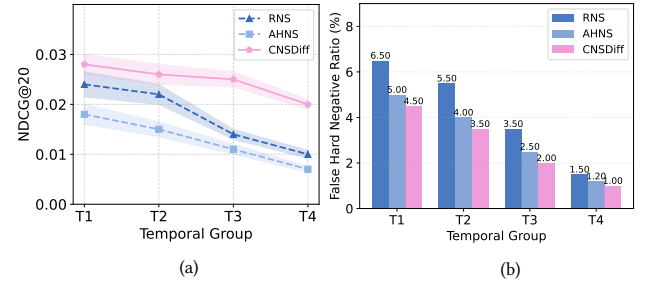


Figure 6: Performance and false hard negative ratio Across different temporal groups.

A.3 Derivation of the Causal Regularization Term.

Eq. (17) can be further reformulated into the following global variational form:

$$\begin{aligned} &\log p_\theta(z_T | \text{do}(z_0), E = e) \\ &\geq \mathbb{E}_{q_\phi(e)} \left[\sum_{t=0}^{T-1} \log p_\theta(z_{t+1} | z_t, e) + \log \frac{p_\theta(e | \text{do}(z_0))}{q_\phi(e)} \right]. \end{aligned}$$

The second term inside the expectation can be decomposed as:

$$\mathbb{E}_{q_\phi(e)} \left[\log \frac{p_\theta(e | \text{do}(z_0))}{q_\phi(e)} \right] = -D_{\text{KL}} \left(q_\phi(e) \| p_\theta(e | \text{do}(z_0)) \right),$$

which naturally introduces a KL divergence as a global regularization term enforcing alignment between the variational posterior and the interventional distribution over environment variables. In practice, since the diffusion model follows a Markov process, we only require pairwise transitions (z_{t-1}, z_t) and the final state z_T . Therefore, the variational approximation can be locally applied as:

$$D_{\text{KL}} \left(q_\phi(z_t | z_{t-1}, e) \| p_\theta(z_t | z_{t-1}, e) \right),$$

which ensures consistency between the learned transition dynamics and the generative model at each step. Furthermore, the term

$$\mathbb{E}_{q_\phi(e)} [\log p_\theta(z_T, e | \text{do}(z_0))]$$

in the ELBO can be decomposed into:

$$\sum_{t=0}^{T-1} \mathbb{E}_{q_\phi(e)} [\log p_\theta(z_{t+1} | z_t, e)] + \mathbb{E}_{q_\phi(e)} [\log p_\theta(e | \text{do}(z_0))],$$

which enables a practical approximation of the interventional log-likelihood $\log p_\theta(z_T | \text{do}(z_0), E)$, while simultaneously minimizing the global KL divergence:

$$D_{\text{KL}} \left(q_\phi(e) \| p_\theta(e | z_T, \text{do}(z_0)) \right).$$

This formulation unifies both the generative reconstruction loss and causal regularization into a coherent variational framework for robust, deconfounded learning.

B DATASET AND PROCESSING DETAILS

Table 3 summarizes the key statistics of each dataset, including the number of users, items, interactions, and the corresponding sparsity levels. Below, we provide a brief introduction to each dataset:

Algorithm 1 Training Procedure of CNSDiff

Input: User-item interaction data $\{(u, v)\}$, model hyperparameters
Output: Trained model parameters θ

- 1: **for** each training epoch **do**
- 2: Compute user embeddings u and item embeddings z_0 via GCN; treat z_0 as the initial state for diffusion
- 3: Construct diffusion input set \mathcal{D}_t by sampling negatives with varying hardness levels via Eq. (14)
- 4: Select hardest negative e_h with maximum inner product with u from \mathcal{D}_{h_t} via Eq. (20)
- 5: Mix e_h with a random negative e_r to generate synthetic negative
- 6: Align the synthetic negative to the item semantic space via Eq. (22)
- 7: Compute the total loss $\mathcal{L}_{\text{total}}$ via Eq. (23)
- 8: Update model parameters: $\theta \leftarrow \theta - \eta \cdot \nabla_{\theta} \mathcal{L}_{\text{total}}$
- 9: **end for**

Table 3: Detailed statistics for each dataset. For each negative sampling method, we conduct 50 epochs per dataset and measure the average runtime per epoch.

Dataset	#Users	#Items	#Interactions	Density
Food	7,809	6,309	216,407	4.4×10^{-3}
KuaiRec	7,175	10,611	1,153,797	1.5×10^{-3}
Yelp2018	8,090	13,878	398,216	3.5×10^{-3}

Table 4: Running Time Comparison.

Datasets	RNS	AHNS	MixGCF	CNSDiff
Food	0.41 s	4.28 s	4.98 s	2.74 s
Yelp2018	1.01 s	8.72 s	10.01 s	7.04 s
KuaiRec	3.04 s	36.98 s	31.06 s	19.58 s

- **Food:** This dataset contains over 230,000 recipes along with millions of user interactions, such as reviews and ratings. It is well-suited for studying user preferences and developing food-related recommendation systems.
- **KuaiRec:** Collected from the Kuaishou platform, this fully-observed dataset includes dense user-item interaction logs with minimal missing data, making it ideal for analyzing the effects of exposure bias and data sparsity in recommendation tasks.
- **Yelp2018:** Comprising user reviews, ratings, and business metadata, this dataset is widely used for recommendation and user behavior modeling.

Preprocessing Details. To ensure data quality, we apply filtering criteria as follows: Users with fewer than 15 interactions are removed from the Food dataset, and users with fewer than 25 interactions are excluded from Yelp2018. Items with fewer than 50 interactions are also filtered out from these datasets. Interactions rated 4 or higher are considered positive samples. For KuaiRec, we consider interactions with a watch ratio of 2 or greater as positive signals. We construct three typical types of out-of-distribution (OOD) scenarios across these datasets:

- **Popularity Shift:** To simulate changes in item popularity, we randomly sample 20% of interactions to form the OOD test set, ensuring a uniform popularity distribution. The remaining interactions are split into training, validation, and IID test sets in a 7:1:2 ratio. This setting is applied to Yelp2018.
- **Temporal Shift:** To capture temporal dynamics, we sort interactions chronologically for each user and select the most recent 20% as the OOD test set. The remaining interactions are divided into training, validation, and IID test sets using a 7:1:2 split. This shift setting is applied to the Food dataset.
- **Exposure Shift:** For KuaiRec, the fully-exposed small matrix is used as the OOD test set, while the larger matrix collected from the online platform is split into training, validation, and IID test sets (7:1:2). This setting captures the distribution shift caused by differing exposure mechanisms.

C HYPERPARAMETERS SETTINGS

We implement our CNSDiff model using PyTorch, and all experiments are conducted on a single NVIDIA RTX 6000 GPU with 48 GB of memory. Following the default settings of the baselines, we set the embedding dimension to 64 and the number of convolution layers to 32 for all models to ensure a fair comparison. For MixGCF, DNS(M,N), and AHNS, the size of the candidate pool for negative sampling is set to 32. We tune the hyperparameters of CNSDiff as follows:

- The number of steps T : [10, 20, 50, 100, 200]
- Regularization coefficient λ_2 : [1e-6, 1e-3, 5e-2, 1e-1, 5e-1]
- Regularization coefficient λ_3 : [1e-6, 1e-3, 5e-2, 1e-1, 5e-1]

We report the impact of different combinations of α and β on model performance in Table 5. In general, the model achieves optimal performance when using the combinations of $[\alpha, \beta] = [2, 8]$ and $[9, 1]$.

D BASELINES

We compare CNSDiff with three types of baseline methods in terms of performance.

Negative sampling methods.

- **RNS** [10] is a simple yet efficient baseline that randomly selects unobserved user-item pairs as negatives.
- **DNS (M, N)** [25] dynamically selects the hardest M negatives from N randomly sampled candidates to better approximate top- K ranking objectives and enhance training effectiveness.
- **MixGCF** [8] enhances collaborative filtering by mixing multiple graph convolutional paths with different propagation ranges, enabling more expressive user and item representations and improving recommendation performance.
- **AHNS** [11] adaptively selects negative samples with appropriate hardness levels during training, effectively mitigating false positive and false negative issues caused by fixed-hardness sampling strategies and improving recommendation performance.
- **DMNS** [23] introduces a conditional diffusion-based multi-level negative sampling strategy that generates negative nodes with controllable hardness levels from the latent space, enabling more effective contrastive learning for graph link prediction.

Distribution shift-aware methods.

Table 5: Performance under different initial and final values of α and β

Dataset	Initial $[\alpha, \beta]$	Final $[\alpha, \beta]$	R@10	N@10	R@20	N@20
Yelp2018	[0.1, 9.9]	[1, 9]	0.0105	0.0069	0.0163	0.0091
	[1, 9]	[5, 5]	0.0099	0.0068	0.0163	0.0091
	[2, 8]	[9, 1]	0.097	0.0065	0.0161	0.0090
KuaiRec	[0.1, 9.9]	[9.9, 0.1]	0.0900	0.5516	0.1357	0.4673
	[1, 9]	[5, 5]	0.0891	0.5530	0.1388	0.4688
	[2, 8]	[9, 1]	0.0909	0.5572	0.1384	0.4678
Food	[0, 10]	[10, 0]	0.0304	0.0219	0.0497	0.0287
	[1, 9]	[5, 5]	0.0301	0.0217	0.0493	0.0285
	[2, 8]	[9, 1]	0.0304	0.0225	0.0496	0.0290

Table 6: Running Time Comparison.

Datasets	RNS	AHNS	MixGCF	CNSDiff
Food	0.41 s	4.28 s	4.98 s	2.74 s
Yelp2018	1.01 s	8.72 s	10.01 s	7.04 s
KuaiRec	3.04 s	36.98 s	31.06 s	19.58 s

- **CDR** [29]: Employs a temporal variational autoencoder to capture preference shifts and learns sparse influences from various environments.
- **InvCF** [41]: Targets the popularity bias by learning disentangled representations of user preferences and item popularity, without relying on predefined popularity distributions.
- **AdvInfoNCE** [40]: An enhanced contrastive learning method that incorporates hardness-aware ranking criteria to improve the model’s generalization in recommendation.
- **DR-GNN** [27]: A graph neural network-based approach for out-of-distribution recommendation, leveraging distributionally robust optimization to handle data distribution shifts.

Diffusion-based methods.

- **DiffRec** [30]: A diffusion-based recommendation framework that learns robust user and item representations by simulating preference propagation through a stochastic diffusion process on the user-item graph.
- **HDRM** [39]: introduces a hyperbolic diffusion framework for recommendation, leveraging the geometric properties of hyperbolic space to preserve anisotropic and directional structures, enhancing the expressiveness of latent representations.
- **CausalDiff** [45] mitigates the impact of environmental confounders by integrating causal inference with diffusion-based representation learning, enabling the model to learn environment-invariant user-item representations for OOD recommendation.

E DISTINCTION FROM EXISTING DIFFUSION-BASED RECOMMENDATION METHODS

In this section, we further discuss the connections and distinctions between **CNSDiff** and existing *diffusion-based recommendation methods*, highlighting the unique advantages of our proposed framework.

E.1 Connections to Diffusion-based Methods

Diffusion models have recently been explored in recommendation systems for robust representation learning [45, 46], graph denoising [49], and sequential modeling [13, 19]. Similar to these works, **CNSDiff** employs a conditional diffusion process to synthesize representations in the latent space. However, unlike models such as DiffRec [32] or HDRM [23], which focus on improving user/item embeddings or interaction modeling, CNSDiff is the first to leverage diffusion *explicitly for negative sample generation*, with controllable hardness via diffusion steps.

E.2 Key Differences and Innovations

Compared to prior diffusion-based methods, **CNSDiff** introduces the following key innovations:

- **Targeted Purpose:** Existing methods typically apply diffusion for embedding enhancement or data augmentation. In contrast, CNSDiff utilizes diffusion as a generative mechanism for constructing *informative and hardness-controllable* negative samples, aligning more directly with the training objective.
- **Causal Regularization:** CNSDiff uniquely incorporates a causal regularization term based on the backdoor criterion, which explicitly mitigates spurious correlations induced by latent environmental confounders—a factor ignored by conventional diffusion-based models.
- **FHNS Mitigation:** Unlike prior methods that may still suffer from false hard negatives (FHNS) under distribution shifts, CNSDiff not only generates negatives from a principled latent distribution but also enforces *environment-invariant generation*, enhancing robustness and generalization.

E.3 Empirical Advantages

As shown in Table 1, CNSDiff consistently outperforms other diffusion-based baselines, including DiffRec, HDRM, and CausalDiff, across three real-world datasets. Specifically:

- CNSDiff achieves an **average performance gain of 13.96%** in Recall and NDCG metrics over state-of-the-art diffusion-based methods.
- Figure 5 shows that CNSDiff maintains a **lower false hard negative ratio** throughout training, leading to faster convergence and more robust generalization.

These results demonstrate that simply applying diffusion modeling is insufficient under distribution shift. Instead, **explicitly modeling causal structures and mitigating confounding effects is essential** for robust recommendation in the wild.